Supporting information:

Codoped perovskite nanocrystals for multiplexed anticounterfeiting applications

Manoj Sharma[1]*, Chang Cao[1], Gaveshana. A. Sepalage[1], Shi Tang[2], Lan Nguyen[1], Hao Deng[1,3], Naufan Nurrosyid[1], Junlin Yan[1], Josh Moon[1], Tuncay Alan[3], James Andell Hutchison[2], Paul Mulvaney[2], Jacek. J. Jasieniak[1]*

[1] Department of Materials Science and Engineering, Monash University, Clayton, Victoria 3800, Australia;

[2] School of Chemistry and ARC Centre of Excellence in Exciton Science, University of Melbourne, Parkville, VIC, 3010 Australia;

[3]Department of Mechanical and Aerospace Engineering, Monash University, Clayton, Victoria 3800, Australia

E-mail: manojsharma@monash.edu;

Jacek.Jasieniak@monash.edu

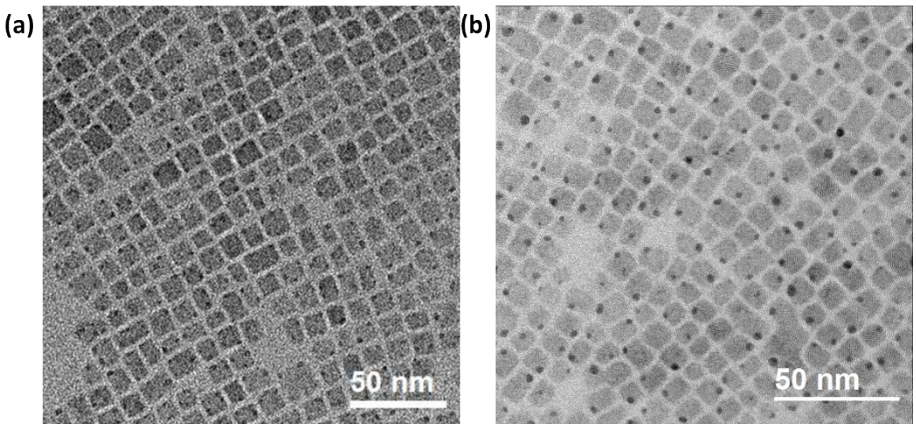

Figure S1. (A-B) TEM images for undoped and Mn-doped $CsPbCl_3$ NCs.

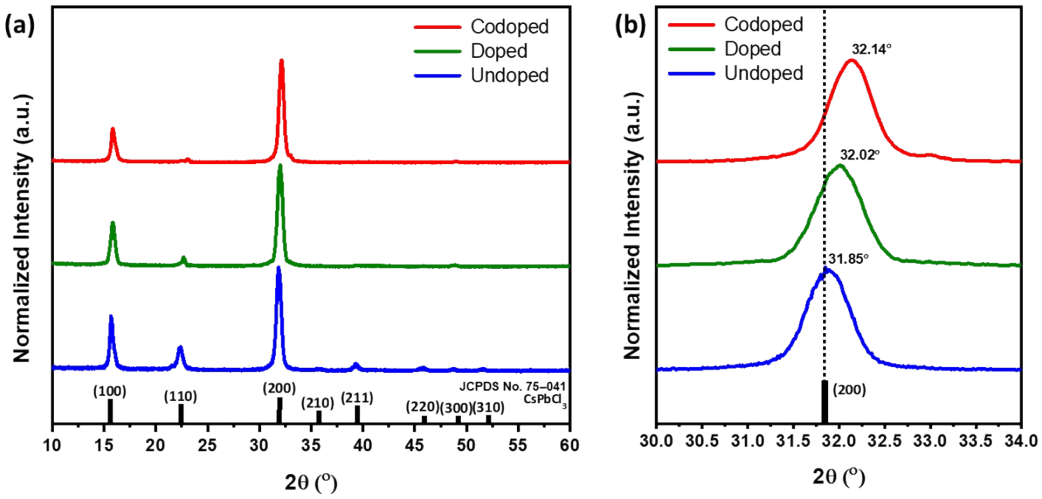

Figure S2. XRD for codoped, doped and undoped $CsPbCl_3$ NCs.

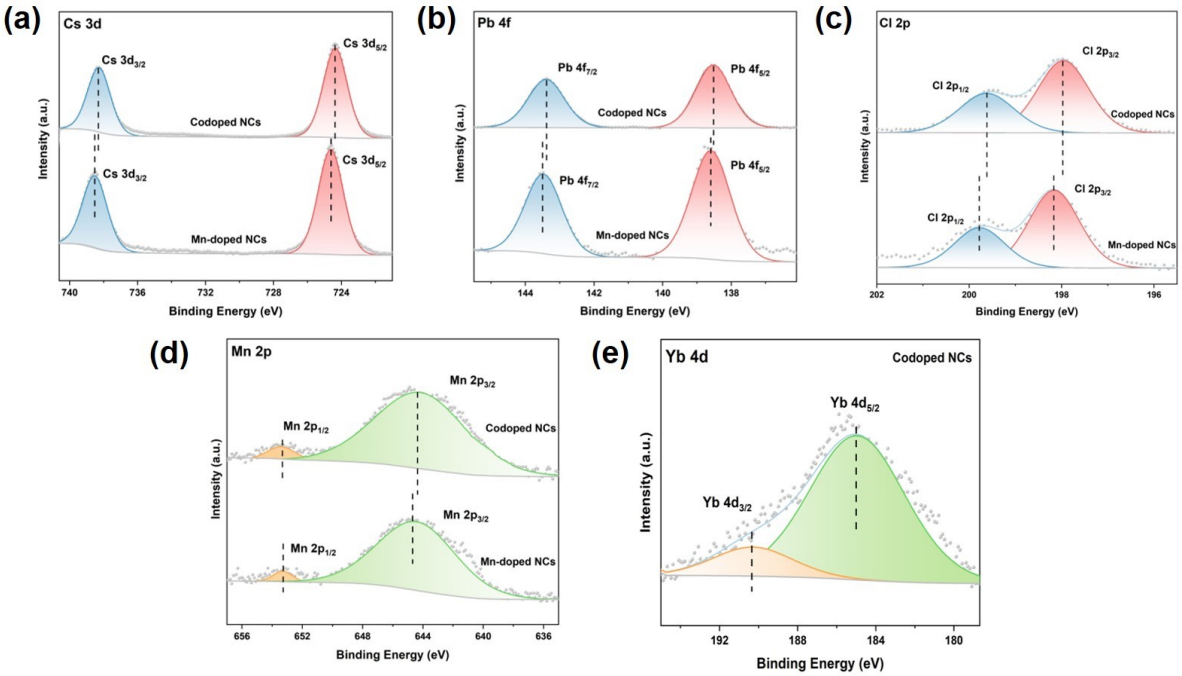

Figure S3. High-resolution XPS spectra for Cs (3d), Pb (4f), Cl(2p), Mn (2p), and Yb (4d) orbitals for doped and codoped $CsPbCl_3$ NCs.

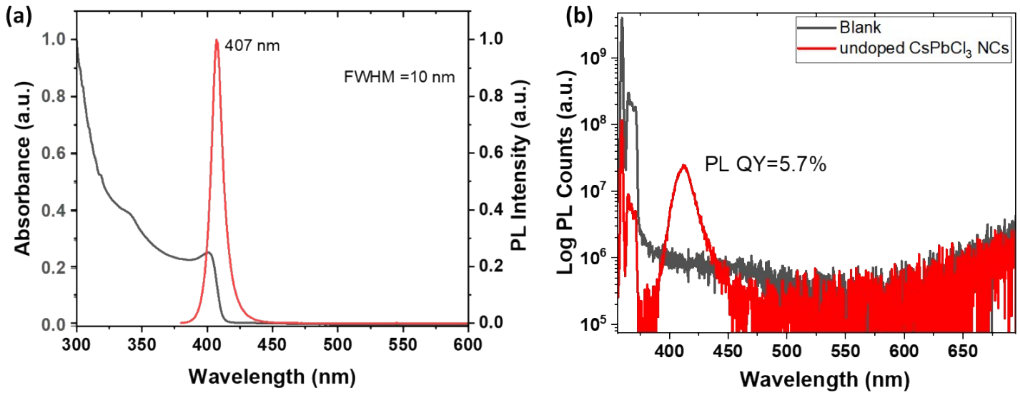

Figure S4. (a) UV-visible absorbance and PL emission for undoped $CsPbCl_3$ NCs. (b) PL Quantum efficiency for undoped $CsPbCl_3$ NCs.

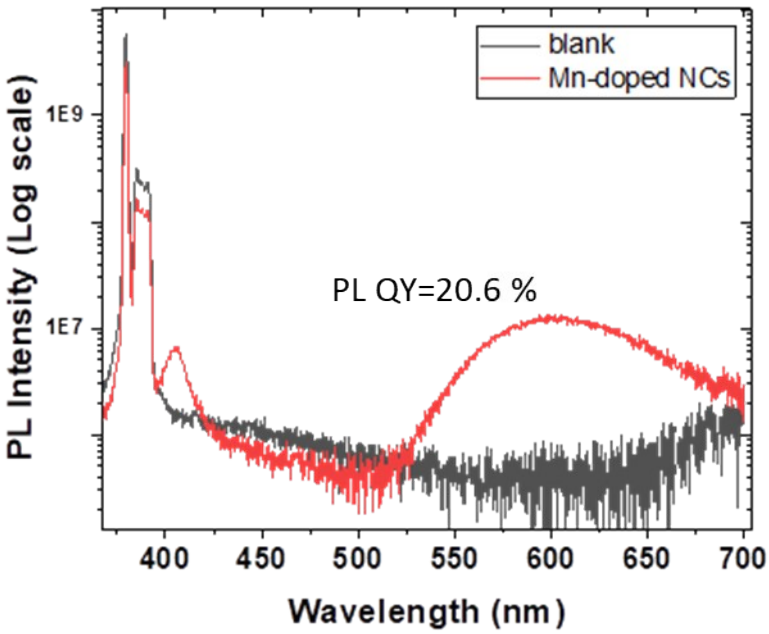

Figure S5: PL Quantum efficiency measured for the visible region for Mn-doped $CsPbCl_3$ NCs.

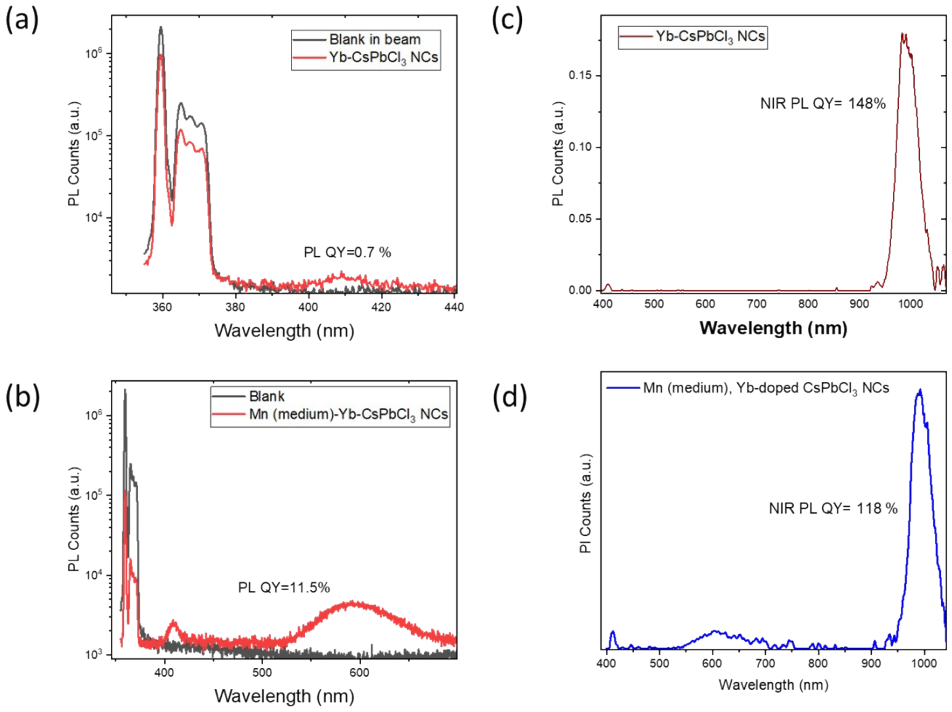

Figure S6: (a, b) PL Quantum efficiency measured for the visible region for Yb-doped and Yb-Mn codoped $CsPbCl_3$ NCs. (c-d) PL spectra were recorded with a calibrated detector in the region of 300-1070 nm. Relative PL QY of the NIR region is estimated as ~148 % and ~118 % for Yb-doped and Yb-Mn codoped NCs, respectively.

TableS1. Details related to the fitting of decay curves for BE emissions

Band edge emission	A_1	A_2	A_3	τ_1 (ns)	τ_2 (ns)	τ_3 (ns)	$\tau_{average}$ (ns)
$CsPbCl_3$ (410 nm)	0.12	89.3	3.55	16.65	4.15	0.63	6.85
$CsPbCl_3$: Mn (410 nm)	313.76	1968.53	12349.37	7.95	1.13	0.23	3.01
$CsPbCl_3$: Mn, Yb (410 nm)	15.75	23.1	72	4.05	0.45	0.08	0.73

TableS2. Details related to the fitting of decay curves for Mn and Yb emissions

Dopant emission	A_1	A_2	τ_1 (ms)	τ_2 (ms)	$\tau_{average}$ (ms)
$CsPbCl_3$: Mn (600 nm)	1.50	7.61	6.30	1.68	1.60

$CsPbCl_3$: Yb, Mn (600 nm)	15.41	41.79	4.66	1.33	1.23
$CsPbCl_3$: Yb, Mn (990 nm)	1.80	7.83	6.4	2.13	2.04

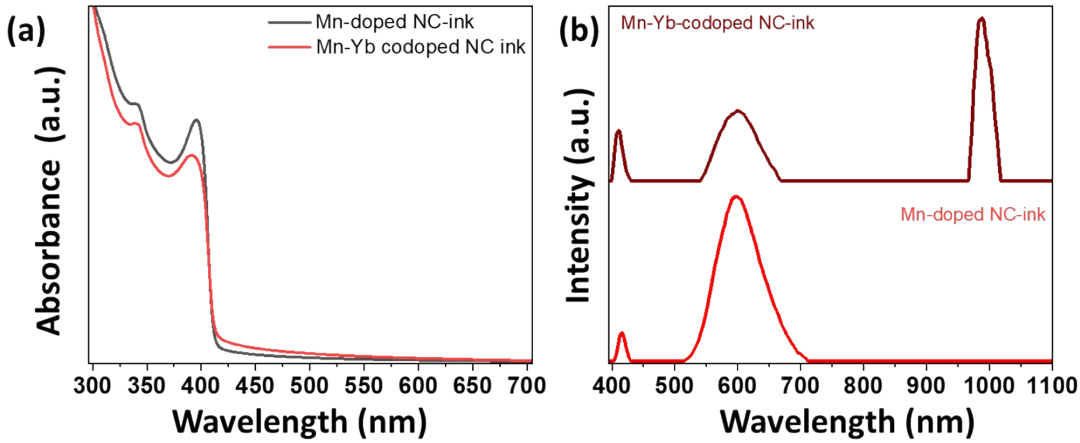

Figure S7. UV-visible absorbance and PL emission for EVA-based Mn-doped and Mn-Yb codoped $CsPbCl_3$ NC inks.

Figure S8. Stability as a function of time for storage in ambient.

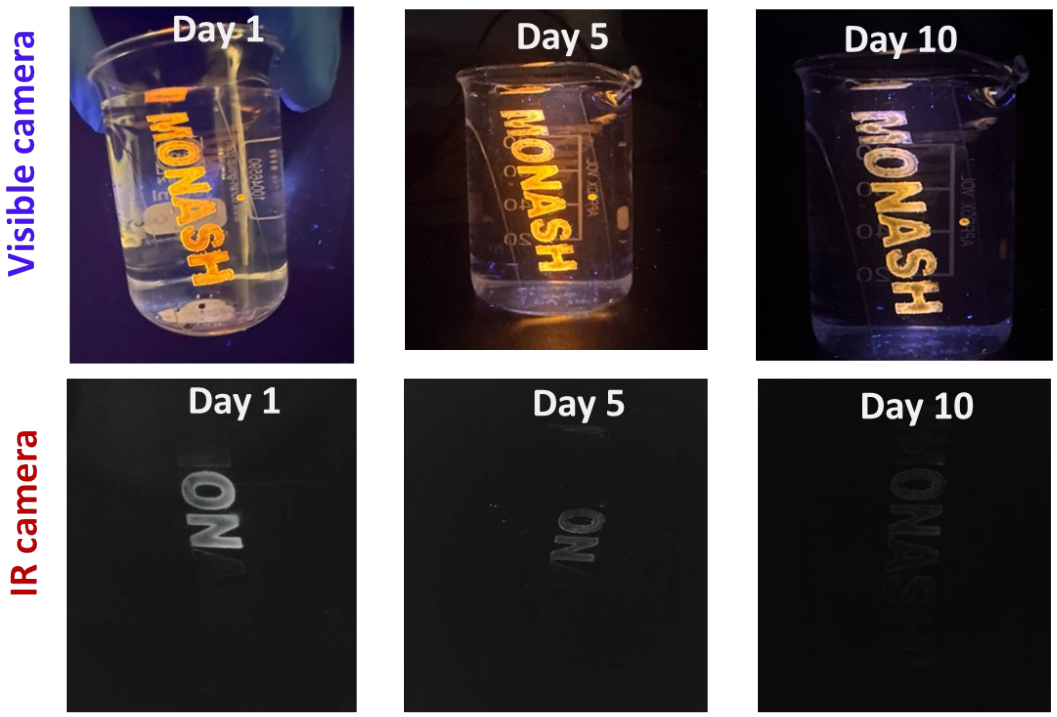

Figure S9. Digital images using visible and IR cameras for NC patterns in water at different intervals.

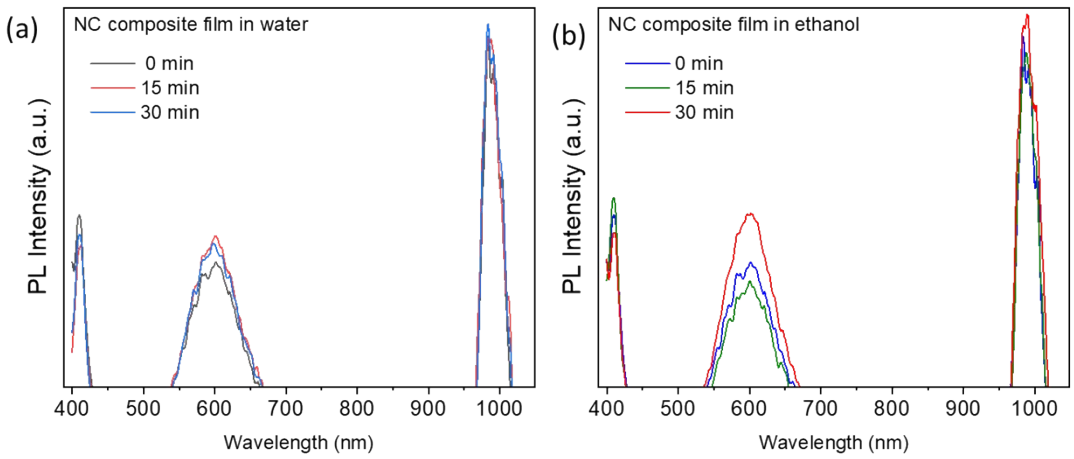

Figure S10. PL emission spectra of codoped NC-EVA composites exposed to different solvents. In contrast, the PL emission spectra for bare NCs are diminished within one minute of exposure to both water and ethanol.

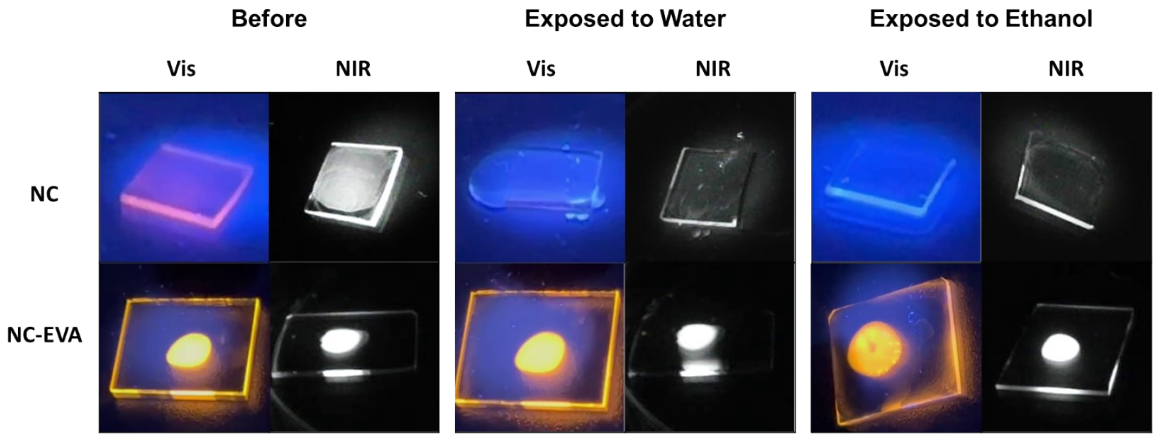

Figure S11. Digital images for bare Mn-Yb codoped NCs and Mn-Yb codoped NCs-EVA composite with visible and IR camera before and after dipping with water and ethanol and recorded at the same time frame.

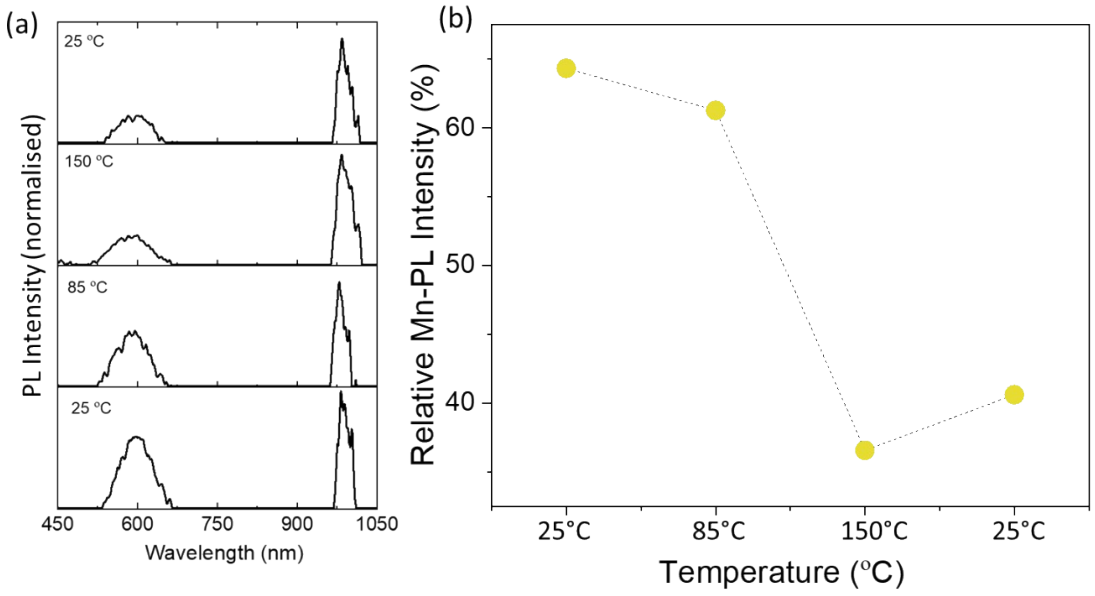

Figure S12. (a) Normalised PL emission spectra of NC composite at different temperatures. (b) Relative PL intensity for Mn-emission is calculated with respect to total integrated PL intensity.

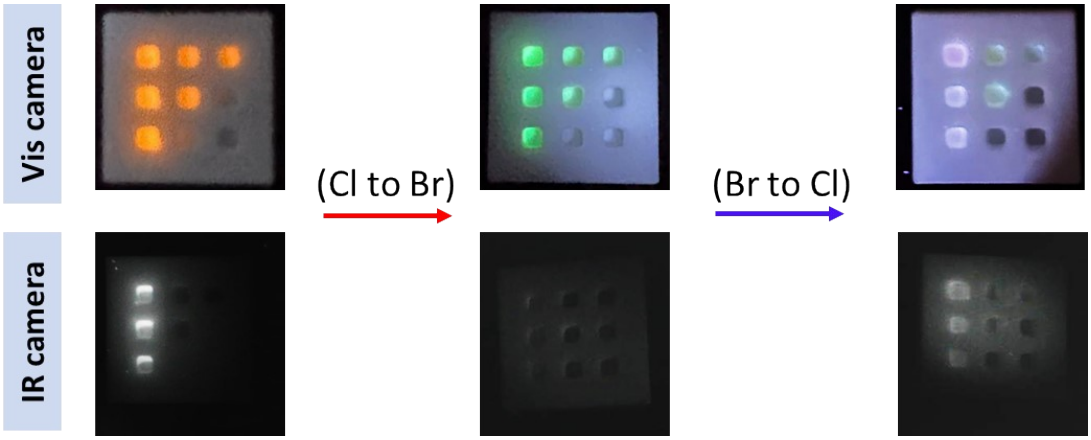

Figure S13. Halide exchange reactions to erase and partially re-activate the secret encrypted information. Square boxes filled with a combination of doped and codoped NC inks. (left to right) digital images under the visible camera and IR camera coupled with a visible long pass filter for NC pattern undergoing anion exchange from Cl to Br and then Br to Cl.